Optical spectroscopy of single quantum dots at tunable positive, neutral, and negative charge states

D. V. Regelman, E. Dekel, D. Gershoni, and E. Ehrenfreund
Physics Department and Solid State Institute, Technion–Israel Institute of Technology, Haifa 32000, Israel

A. J. Williamson, J. Shumway, and A. Zunger
National Renewable Energy Laboratory, Golden Colorado 80401

W. V. Schoenfeld and P. M. Petroff
Materials Department, University of California, Santa Barbara, California 93106

We report on the observation of photoluminescence from positive, neutral, and negative charge states of single semiconductor quantum dots. For this purpose we designed a structure enabling optical injection of a controlled unequal number of negative electrons and positive holes into an isolated InGaAs quantum dot embedded in a GaAs matrix. Thereby, we optically produced the charge states -3, -2, -1, 0, $+1$, and $+2$. The injected carriers form confined collective "artificial atoms and molecules" states in the quantum dot. We resolve spectrally and temporally the photoluminescence from an optically excited quantum dot and use it to identify collective states, which contain charge of one type, coupled to few charges of the other type. These states can be viewed as the artificial analog of charged atoms such as H^-, H^{-2}, H^{-3}, and charged molecules such as H_2^+ and H_3^{+2}. Unlike higher dimensionality systems, where negative or positive charging always results in reduction of the emission energy due to electron-hole pair recombination, in our dots, negative charging reduces the emission energy, relative to the charge-neutral case, while positive charging increases it. Pseudo-potential model calculations reveal that the enhanced spatial localization of the hole wave function, relative to that of the electron in these dots, is the reason for this effect.

I. INTRODUCTION

Real atoms and molecules often appear in nature as charged ions. The magnitude and sign of their ionic charge reflects their propensity to successively fill orbitals (the Aufbau principle) and to maximize spin (Hund's rule). As a result they often exhibit only unipolarity (being either negative or positive) and remain in a very restricted range of charge values (e.g., O^0, O^{-1}, O^{-2} or Fe^{+2}, Fe^{+3}, etc.) even under extreme changes in their chemical environments.

Semiconductor quantum dots (QD's) are of fundamental and technological contemporary interest mainly for their similarities to the fundamental building blocks of nature (they are often referred to as "artificial atoms"[1–3]) and because they are considered as the basis for new generations of lasers,[4] memory devices,[5] electronics,[6] and quantum computing.[7]

Unlike their atomic analogs, however, semiconductor QD's exhibit large electrostatic capacitance, which enables a remarkably wide range of charge states. This has been demonstrated by carrier injection either electronically[6,8,9] by scanning tunneling microscopy,[10] or even optically.[11,12] This ability to variably charge semiconductor QD's makes it possible to use them as a natural laboratory for studies of inter-electronic interactions in confined spaces and at the same time it creates the basis for their potential applications. Two physical quantities are of particular importance when quantum dot charging is considered: (i) The charging energy $\mu_N = E_N - E_{N-1}$ required to add a carrier to a QD containing already $N-1$ "spectator" carriers. Measurements[2,6,8,10] and calculations[13,14] of QD charging energies have revealed deviations from the Aufbau principle and Hund's rule, in contrast with the situation in real atoms.[14] (ii) The electron-hole (e-h) recombination energy $\Delta E_{eh}(N_e, N_h)$ in the presence of N_e-1 and N_h-1 additional "spectator" electrons and holes. (ΔE_{eh} is of great importance for research and applications which involve light, because light emission from QD's originates from the recombination of an e-h pair). Measurements of $\Delta E_{eh}(N_e, N_h)$ were so far carried out only for neutral[15] and negatively charged[8,11,16] QD's. It was found that upon increasing the number of electrons and e-h pairs, $\Delta E_{eh}(N_e, N_h)$ decreases, i.e., the emission due to the e-h radiative recombination shifts to the red.

In higher-dimensional systems adding negative and/or positive charge produces the same effect. This is the case for the positively charged molecule H_2^+ vs H_2 (Ref. 17) in three dimensions (3D), and the positively or negatively charged exciton (the X^+ or X^- trion) vs the exciton, in 2D quantum wells (QW's).[18]

In the present study, we designed a device enabling optical injection of a controlled unequal number of electrons and holes into an isolated InGaAs QD, producing thus the charge states -3, -2, -1, 0, $+1$, and $+2$. The injected carriers form confined collective "artificial atoms and molecules" states in the QD. Radiative e-h pair recombination takes place after such a collective few carrier state relaxes to its ground state. We resolve spectrally and temporally the photoluminescence (PL) from the QD and use it to determine the collective carriers' state from which it originated. In particular, we identify collective states, which contain charge of one type coupled to few charges of the other type. These states can be viewed as the artificial analog of charged atoms such
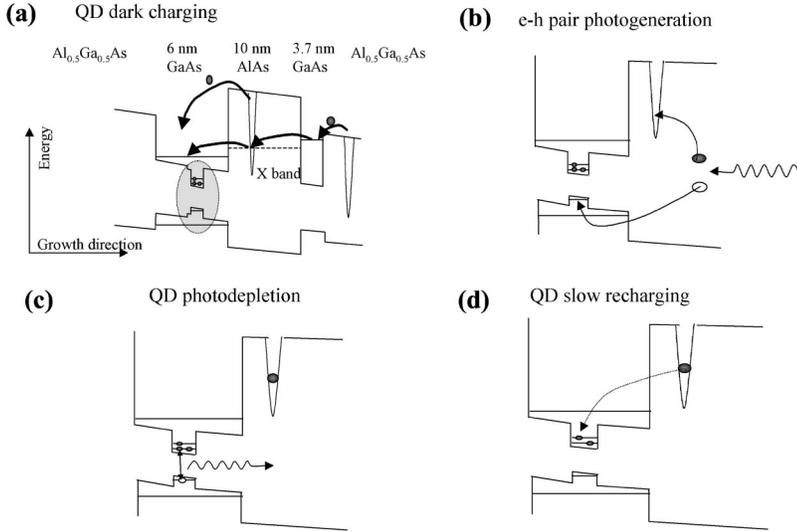
(a) QD dark charging

Al$_{0.5}$Ga$_{0.5}$As   6 nm   10 nm   3.7 nm   Al$_{0.5}$Ga$_{0.5}$As
GaAs   AlAs   GaAs

Energy

X band

Growth direction

(b) e-h pair photogeneration

(c) QD photodepletion

(d) QD slow recharging

FIG. 1. Schematic description of the mixed type SAQD sample. (a) Initial charging of the QD with electrons from ionized donors, (b) *e*-*h* pair photogeneration, (c) QD photodepletion, and (d) QD slow recharging by the captured electron from the ionized donor.

as H$^-$, H^{-2}, H^{-3}, and charged molecules such as H$_2^+$ and H$_3^{+2}$.[17] We demonstrate that, unlike the case in negatively charged QD's, and unlike higher dimensionality charged collective states, positively charged dots show an increase in E_{eh} so the emission due to radiative recombination of an *e*-*h* pair shifts to the blue.

Many-body pseudopotential calculations reveal that this trend originates from the increased spatial localization of the hole wave function with respect to that of the electron. The calculations tend to agree with the measured results. They can essentially be summarized as follows: The energy associated with hole-hole repulsion is larger than the energy associated with electron-hole attraction, while the latter is larger than the energy associated with electron-electron repulsion.[19] Therefore, in the presently studied QD's, as already alluded to by Landin *et al.*,[13] excess electrons decrease (red shift) the recombination energy, while excess holes increase (blueshift) it.

II. SAMPLES AND EXPERIMENTAL RESULTS

We have prepared the semiconductor QD's by self-assembly. We used molecular beam epitaxy (MBE) to grow InAs islands on GaAs by exploiting the 7% lattice mismatch strain driven change from epitaxial to islandlike growth mode.[20] This growth mode change occurs after the GaAs surface is covered with 1.2 monolayers of InAs. During the growth of the InAs islands, the sample was not rotated. Therefore, the density of the islands varies across the sample surface, depending on the distance from the In and As MBE elemental sources. In particular, one can easily find low-density areas, in which the average distance between neighboring islands is $\simeq \mu$m. This distance, which is larger than the resolution limit set by the diffraction at the optical emission wavelength of these islands, permits PL spectroscopy of individual single islands.[15]

The self-assembled InAs islands were partially covered by deposition of a 2–3 nm thick epitaxial layer of GaAs. The growth was then interrupted for a minute, to allow melting of the uncovered part of the InAs islands and diffusion of In

(Ga) atoms from (into) the strained islands.[21] A deposition of GaAs cap layer terminated the growth sequence. The QD's thus produced are of very high crystalline quality, their typical dimensions are 40 nm base and 3 nm height. They form deep local potential traps for both negative (electrons) and positive (holes) charge carriers.

Our self-assembled quantum dots (SAQD's) (Refs. 15,22) and similar other QD systems were very intensively studied recently using optical excitation and spectral analysis of the resulting PL emission from single QD's.[3,8,11,13,16,23,24] These studies established both experimentally and theoretically that the number of carriers, which occupy a photoexcited QD, greatly determines its PL spectrum.

Since optical excitation is intrinsically neutral (electrons and holes are always photogenerated in pairs), it is not straightforward to use it for investigating charged QD's.[8] Two innovative methods have been recently used to optically charge QD's. The first utilizes spatial separation of photogenerated electron hole (*e*-*h*) pairs in coupled narrow and wide GaAs QW's, separated by a thin AlAs barrier layer.[5] In this case, the lowest energy conduction band in the AlAs barrier (*X* band) is lower than the conduction band of the narrow QW, but higher than that of the wide one. As a result, electrons preferentially tunnel through the barrier and accumulate in the SAQD's within the wider well, while holes remain in the narrow QW [see Fig. 1(a)]. The second method utilizes capture of photogenerated electrons by ionized donors [see Fig. 1(b)–1(d)].[11] In this case, the holes quickly arrive at the QD's, while the captured electrons slowly tunnel or hope from the donors to the QD's, thereby effectively charging or discharging the QD's during the photoexcitation. In this work, we combined these two methods to effectively use the excitation density in order to control the number of electrons present in the QD when radiative recombination occurs (see Fig. 1).

Two samples were investigated. Sample A, which is used here as a control, neutral sample, consists of a layer of low density In(Ga)As SAQD's embedded only within a thick layer of GaAs.[22] Sample B, which we used for optical charging, consists of a layer of similar SAQD's, embedded within
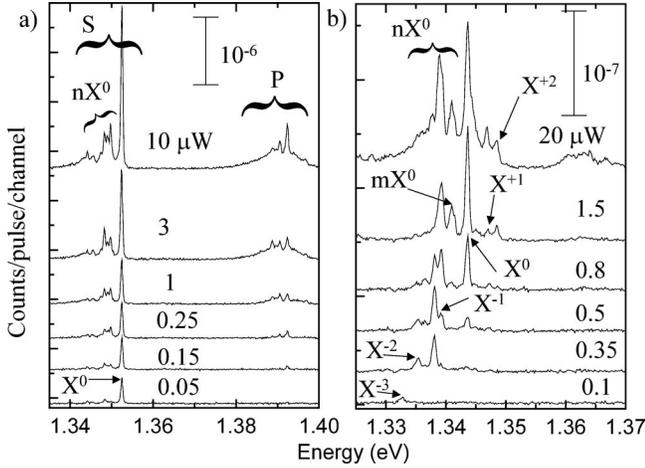
FIG. 2. Picosecond pulse excited photoluminescence spectra of single QD's for increasing excitation intensities. (a) From a charge-neutral QD (the control sample A) and (b) from a charged QD (mixed type sample B). The discrete PL lines due to the recombination of neutral excitons (X^0, nX^0), negatively charged (X^{-i}) and positively charged (X^{+i}) excitons are marked in the figures.
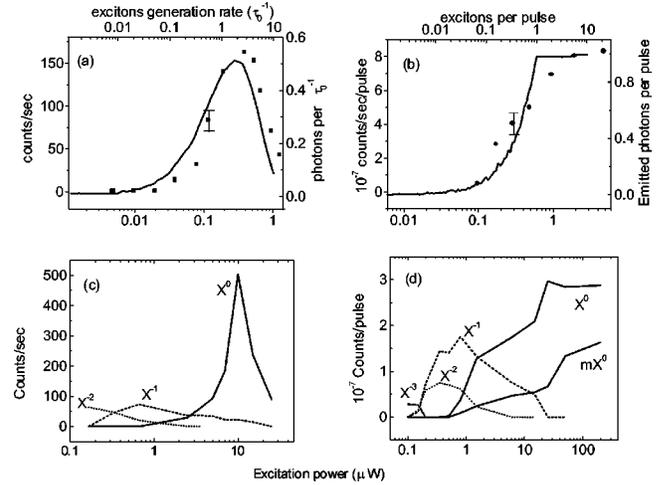

FIG. 3. Spectrally integrated photoluminescence intensity of the various spectral lines as a function of excitation intensity (in the integration, possible "fine" structure of the spectral lines is ignored and background due to neighboring lines is subtracted using a Gaussian line fitting procedure). (a) The neutral (X^0) line from the control sample A at cw excitation. (b) Same as (a) at pulsed excitation. The solid lines in the figures (upper and right hand side axes, where τ_0 is the radiative lifetime of e_1-h_1 pair) represent our rate equation model calculations (Ref. 22). Note the typical difference between cw and pulsed excitation. Whereas in the first case the PL intensity goes through a clear maximum and then it decreases with further increase of the excitation density, in the second case it saturates and remains constant. The intensity dependence of the negatively charged and the neutral PL lines from the mixed type QD sample B, for cw and for pulse excitations are given in (c) and (d), respectively. Note the clear distinction between the intensity dependence of the PL lines due to negatively charged states and those due to neutral states. We use these differences to determine the origin of the various PL lines (see text).

the wider of two coupled GaAs QW's, separated by a thin AlAs barrier layer.[5]

We spatially, spectrally and temporally resolved the PL emission from single SAQD's in both samples using a variable temperature confocal microscope setup.[15] Figure 2 compares the pulse excited PL spectra of the neutral [Fig. 2(a)] and mixed type [Fig. 2(b)] samples. The excitation in both pulse and cw (not shown here) excitations was at photon energy of 1.75 eV and the repetition rate of the picosecond pulses was 78 MHz ($\simeq 13$ ns separation between pulses). In Fig. 3 we present the spectrally integrated PL emission intensity from the various spectral lines of Fig. 2, as a function of the excitation intensity for cw [Figs. 3(a) and 3(c)] and pulse excitation [Figs. 3(b) and 3(d)]. By comparing the PL spectra from the neutral sample (A) to that from the charged one (B) and by comparing the cw PL spectra to its pulsed evolution as we increased the excitation power, we identified the various discrete spectral lines in the spectra. They are marked in Fig. 2 by the collective carriers' state from which they resulted.

III. DISCUSSION

We interpret the evolution with excitation intensity as follows: At very low cw excitation intensities of neutral QD, there is a finite probability to find only one electron-hole (e-h) pair at their lowest energy levels e_1,h_1 (the analog of an S shell of atoms) within the QD. The radiative recombination of the e-h pair (exciton) gives rise to the PL spectral line, which we denote by X^0 (we ignore in this discussion the "fine" exciton structure,[25] which gives rise to the fraction of a meV spectral line splittings observed in Fig. 2). With the increase in the excitation power, the probability to find few e-h pairs within the QD increases significantly. Since each level in the QD can accommodate only two carriers, when three e-h pairs are confined in the QD, the carriers must

occupy the first (e_1,h_1) and second (e_2,h_2) single-particle energy levels. Recombination of carriers from the second level gives rise to the group of spectral lines, which we denote by P, in analogy with the P shell of atoms. The expected fourfold (including spin) degeneracy of the P level of our QD's is removed by the QD's asymmetrical shape. Therefore the spectral range which we denote by P contains two subgroups of lines, typically[22] roughly 6 meV apart. The magnitude of this splitting is in agreement with our theoretical model (see below). At these excitation intensities, satellite spectral lines appear on the lower energy side of the X^0 line. These lines are due to the exchange energies between pairs of same charge carriers that belong to different single particle energy levels (shells). The exchange interaction, reduces the bandgap of the QD (in a similar way to the well known bulk phenomenon of "bandgap renormalization"), and, with the increase in the excitation power, it gives rise to subsequently red shifted satellite PL lines (nX^0), as higher numbers of spectator e-h pairs are present during the radiative recombination.[15,22,23]

Immediately after the optical pulse, excitation intensity dependent number of photogenerated e-h pairs (N_x) reaches the QD. Their radiative recombination process is sequential,

and the e-h pairs recombine one by one. Therefore, all the pair numbers that are smaller than N_x contribute to the temporally integrated PL spectrum. This typical behavior is demonstrated in Fig. 2(a) in which the temporally integrated PL spectra from a single QD of the control sample (A) are presented for various excitation powers. As can be seen in the figure, the PL intensity of all the spectral lines reach maximum and remains constant for further increase in the excitation power. This behavior is well described by a set of coupled rate equations model[22] which can be analytically solved to yield the probabilities to find the photoexcited QD occupied by a given number of e-h pairs.[22] In Fig. 3(b) the measured PL intensity of the X^0 line as a function of the pulse-excitation power is compared with the calculated[22] number of X^0 emitted photons as a function of the number of photogenerated excitons in the QD, for each pulse. We note here that a necessary condition for the above analysis to hold is that the pulse repetition rate is slow enough, such that all the photogenerated pairs recombine before the next excitation pulse arrives.

When cw excitation is used, the evolution of the temporally integrated PL spectra with the increase in excitation intensity is different. In this situation, the probability to find a certain number of e-h pairs within the QD reaches a steady state. The higher the excitation power is the higher is the probability to find large numbers of e-h pairs in the QD, while the probability to find the QD with a small number of pairs rapidly decreases. As a result, all the observed discrete PL lines at their appearance order undergo a cycle in which their PL intensity first increases, then it reaches a well defined maximum, and eventually it significantly weakens. In Fig. 3(a) we compare the measured spectrally integrated PL intensity of the X^0 line as a function of the excitation power, with its calculated emission rate as a function of the photogeneration rate of excitons in the QD.

The PL spectrum from the mixed-type sample B, and its evolution with excitation power is very different. The reason for this difference is the fact that the SAQD's in the mixed-type sample B are initially charged with electrons.[26] These electrons are accumulated in the SAQD's due to the sample design, which facilitates efficient hopping transport of electrons from residual donors. The maximal number of electrons in a given QD is limited by the electrostatic repulsion, which eventually forces new electrons to be unbound, i.e., have energies above the wetting layer continuum onset. We found experimentally that the maximal number of electrons is three, in excellent agreement with our model calculations (see below).

With the optical excitation, the ionized donors separate a certain fraction of the photogenerated e-h pairs. Then, while the donors capture electrons and delay their diffusion,[11] the holes quickly reach the QD's and deplete the QD's initial electronic charge. The recombination of an e-h pair in the presence of a decreasing number of electrons reveals itself in a series of small discrete lines to the lower energy side of the PL line X^0 [Fig. 2(b)]. At very low excitation intensity, a single sharp PL line [which we denote in Fig. 2(b) by X^{-3}] appears. The X^{-3} line originates from the recombination of an e-h pair in the presence of additional three spectator elec-

trons. As can be seen in Fig. 2(b), with the increase in excitation power, new spectral lines appear on the higher energy side of the first to appear line. With increasing intensity, the X^{-3} line weakens and there emerge small higher energy lines (the lowest energy of which is marked by X^{-2}) which originates from pair recombination in the presence of two additional electrons. With further increase of the excitation power these lines lose strength as well and few other spectral lines, at yet higher energy, appear. We mark the strongest line in this group by X^{-1}. At yet higher excitation intensity, a spectral line, which we denote by X^0 emerges. With further increase of the excitation power, new satellite PL lines appear, but now they appear in both the higher and lower energy sides of the neutral, X^0 line of sample B. While the lines to the lower energy side are similar to those observed in the PL spectra from QD's in the control sample (the nX^0 lines), the higher energy lines are entirely different. This difference results from the mechanism of preferential hopping of photoexcited holes into the QD's. This mechanism leads, at high enough intensities, not only to negative charge depletion, but also to positive charging of the QD's.

We thus identify the higher energy satellites of the X^0 line as resulting from e-h recombination in the presence of additional holes within the QD. We attribute the first two higher energy satellites to final states with one (line X^{+1}) and two (line X^{+2}) holes. The positive charging mechanism at high optical excitation power should not come as a surprise, since while the SAQD cannot contain more than three electrons, it can definitely collect holes from a larger number of neighboring photodeionized donors. The high energy side of the X^0 line does not extend over 6 meV and we never observed more than two discernible satellites at this side of the spectrum. As explained below, this does not mean that the QD cannot be charged with a larger number of holes. It reflects the fact that the observed blueshift is maximal for a positively charged QD with only two holes.

The evolution of the spectra with the increase in pulse-excitation power [Fig. 2(b)] is similar to that of the control sample except for one important difference. Here, the PL intensity of all the spectral lines due to recombination from negatively charge states, which appear at low excitation power prior to the appearance of the X^0 line, reaches maximum and then considerably weakens at higher excitation power. The X^0 line is the first spectral line that behaves differently. Its intensity reaches a maximum and remains constant as the excitation power is further increased.

In Fig. 3(c) [Fig. 3(d)] we present the spectrally integrated PL intensity of various spectral lines from a single mixed type QD as a function of the cw (pulse) excitation intensity. The figure demonstrates that the "neutral" PL lines, such as X^0 and nX^0, evolve similarly to those of sample A. Under pulse excitation their intensity reaches a maximum and remains unchanged as the pulse excitation intensity is further increased. At the same time, the negatively "charged" PL lines evolve similar to the lines of sample A under cw-mode excitation. We attribute this difference to the long hopping times of the trapped photoexcited electrons, which determine the lifetime of the emission from the various charged states. This lifetime can be crudely estimated from the intensity

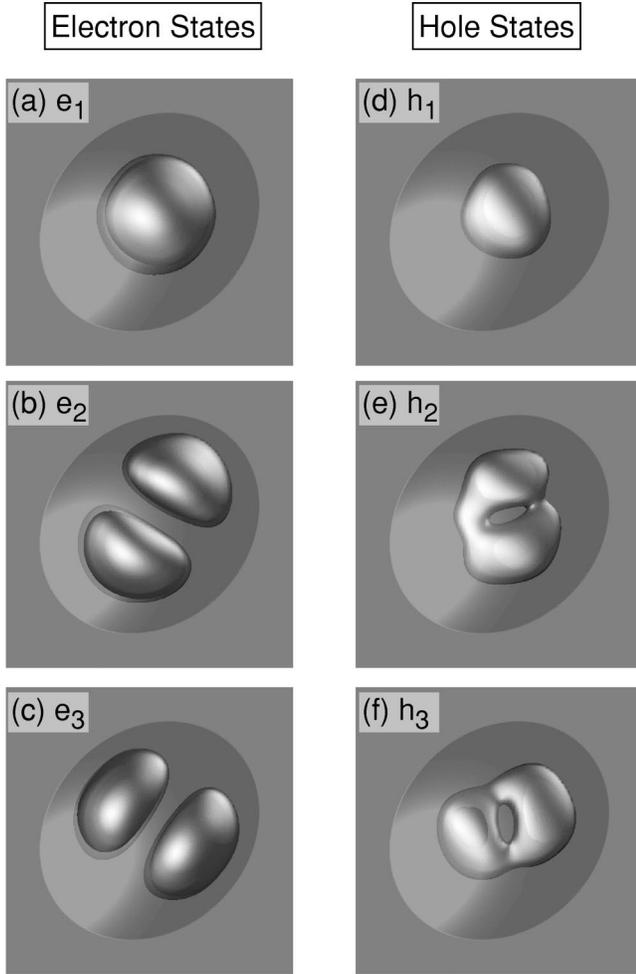| Electron States	Hole States
(a) e_1	(d) h_1
(b) e_2	(e) h_2
(c) e_3	(f) h_3

FIG. 4. Top view of the calculated single electron and hole wave functions squared for the SAQD under study. The isosurfaces contain 75% of the total charge. The pseudopotential calculations use the linear combination of bulk bands method (Ref. 29). Note that the spatial extent of the electron wave function is larger than that of the hole.

ratio between the maximum intensity of the X^0 PL line under cw excitation and that from the negatively charge states [10:1, see Fig. 4(c)], since the emission intensity at maximum is inversely proportional to the state lifetime.[22,27] From the measured decay time of the X^0 line ($\simeq 1.3$ ns, not shown) we deduce the hopping times and find them to be slightly longer than the pulse repetition time ($\simeq 13$ ns). Therefore, under pulsed excitation, once the QD is optically depleted from its initial charge, it remains so for times longer than the time difference between sequential pulses. Thus, PL lines that result from exciton recombination in the presence of negative charge evolve similar to neutral lines under cw-mode excitation [Fig. 3(a)], and their intensity weakens with the increase in excitation power. We use this behavior to sort out the neutral states PL emission from that of negatively charged ones, in general, and for identifying the X^0 line in particular.

The larger the number of deionized donors which participate in the depletion process, the shorter is the lifetime of the charge depleted state that they generate. This can be straight-forwardly deduced from Fig. 3(d) and more quantitatively by simple rate equation model simulations.[27] Since four and five deionized donors are involved in generating the $q = +1$ and $q = +2$ charge states, respectively, the lifetime of these states is shorter than that of the charge-neutral state and shorter from the pulse repetition time. Hence, the evolution of the PL intensity of the X^{+1} and X^{+2} lines with increasing pulse excitation power, is similar to that of the X^0 line.

IV. COMPARISON WITH THEORY

The effect of spectator charges on the recombination energy of the fundamental $e_1 - h_1$ excitonic transitions $\Delta E_{e_1,h_1}^{(N_e,N_h)}$ is theoretically given by:[14]

$$\Delta E_{e_1,h_1}^{(N_e,N_h)} = \left[\varepsilon_{e_1} - \varepsilon_{h_1} - J_{e_1,h_1} \right]$$

$$- \left[\sum_{i=2}^{N_e} \left(J_{e_1,e_i} - J_{h_1,e_i} \right) + \sum_{j=2}^{N_h} \left(J_{h_1,h_j} - J_{e_1,h_j} \right) \right]$$

$$+ \left[\Delta_{\text{exch}}^{(N_e)} + \Delta_{\text{exch}}^{(N_h)} \right] + \Delta_{\text{corr}}^{(N_e,N_h)}. \quad (1)$$

In Eq. (1), the first term in square brackets is the recombination energy of the exciton in the absence of additional carriers. Here ε_{e_1} (ε_{h_1}) is the energy of the first single electron (hole) level and J_{e_1,h_1} is the e-h pair binding energy. The second bracketed term ("Coulomb shift," δE_{Coul}) contains the difference between the Coulomb repulsion and Coulomb attraction terms between the recombining exciton and the spectator electrons and holes. In simple models, in which the electrons and holes have the same single particle wave functions, this term vanishes.[15,22–24] However, if the holes (electrons) are more localized than the electrons (holes), then the Coulomb term results in red (blue) PL shift upon electron (hole) charging.[19] The third bracketed term ("exchange shift" δE_{exch}) is the change in the exchange energies upon charging. The exchange term is always negative for both electrons and holes charging.[22–24] This term is responsible for the multi line PL spectrum, since open shells in the final state give rise to few spin multiplets whose energies depend on the spin orientation of the carriers in these shells. The last term ("correlation shift" δE_{corr}) is due to the difference in correlation between the interacting many carriers within the QD. This term is always negative as well.[29] In higher dimensionality systems, such as quantum wires, wells and bulk semiconductors, the carrier wave functions are delocalized in at least one dimension. Therefore, the Coulomb shift in Eq. (1) is much smaller than the correlation shift. As a result, redshifts are anticipated for both negative and positive charging. In zero dimensional QD's whose dimensions are comparable to and smaller than the bulk exciton radius, the correlation terms are smaller than the Coulomb and exchange terms.[28] Thus, in some cases, a positive Coulomb term may overwhelm the exchange and correlation terms, resulting in blue PL shift upon QD charging.[19] Clearly, a microscopic calculation is needed to establish the detailed balance between the various terms of Eq. (1). We used pseudopotential

calculations[19] in order to realistically estimate the various terms in Eq. (1). The first three terms were obtained via first-order perturbation theory whereas the last term (the correlation energy) was obtained via configuration-interaction calculations.[14,29] The QD calculated here,[22] has a slightly elongated lens shape, with major and minor axis 45 and 38 nm (in the 110 and $\bar{1}10$ directions, respectively), and a height of 2.8 nm. Both the QD's and the two monolayer wetting layer have a uniform composition of $In_{0.5}Ga_{0.5}As$, and they are embedded in a GaAs matrix. The shape, size, and composition are based on experimental estimations, and they are somewhat uncertain.

The pseudopotential treats the alloy atomistically, and it includes spin-orbit interaction and strain. We include the first six bound electron and hole states in our configuration-interaction expansion. The calculated S-P shells splitting ($\varepsilon_{e_2} - \varepsilon_{e_1} + \varepsilon_{h_2} - \varepsilon_{h_1} \simeq 37$ meV), well agrees with the measured one and so does the energy splitting of the P shell ($\varepsilon_{e_3} - \varepsilon_{e_2} + \varepsilon_{h_3} - \varepsilon_{h_2} \simeq 6$ meV).

Figure 4 shows isosurface plots of the calculated density of probability for electrons and holes in their three lowest energy states. The electric charge that these isosurfaces contain amount to 75%. The figure clearly demonstrates that the holes are more localized than the electrons. Quantitatively speaking, the volume of the e_1 isosurface in Fig. 5 (1600 nm^3) is 3 times larger than that of h_1. Consequently, the Coulomb shift term in Eq. (1) contributes a red (blue) shift to the excitonic recombination for negative (positive) charging.

By calculating the carrier addition energies μ_N,[14] we find the energies 1.460, 1.473, 1.500, and 1.510 eV for electron charging of $N=1$, 2, 3, and 4, respectively. Only the first three energies are below the calculated wetting layer conduction band energy of 1.506 eV. This is in perfect agreement with the fact that we never observed experimentally higher then $N=3$ negatively charged QD. Similar calculations for holes yielded that the SAQD can hold at least 6 holes.

In Fig. 5 we compare the measured PL energies due to e_1-h_1 pair recombination from various charged exciton states with the calculated emission. The energy is measured relative to the uncharged e_1-h_1 recombination energy. Shaded bars indicate the measured peak positions. The bar positions are obtained by averaging results of measurements from six different QD's, and the width of the bars represents the statistical and experimental uncertainties. Dashed lines represent the sums of the first three terms of Eq. (1), whereas solid lines represent the full calculations (with the correlation terms).

As can be seen in Fig. 5 the calculations resemble the optical measurements. (i) We see a blueshift for hole charging and a redshift for electron charging. The computed shifts are underestimated relative to experiment. We attribute these discrepancies to uncertainties in SAQD shape, size, and composition profile. (ii) The blueshift due to hole charging is bound from above. It ceases to increase after two or the most three positive charges (depending on whether the last one is an Aufbau or non-Aufbau state). For additional positive charging, the exchange and correlation terms overwhelm the Coulomb term. (iii) We calculate two PL lines for $q=-2$,
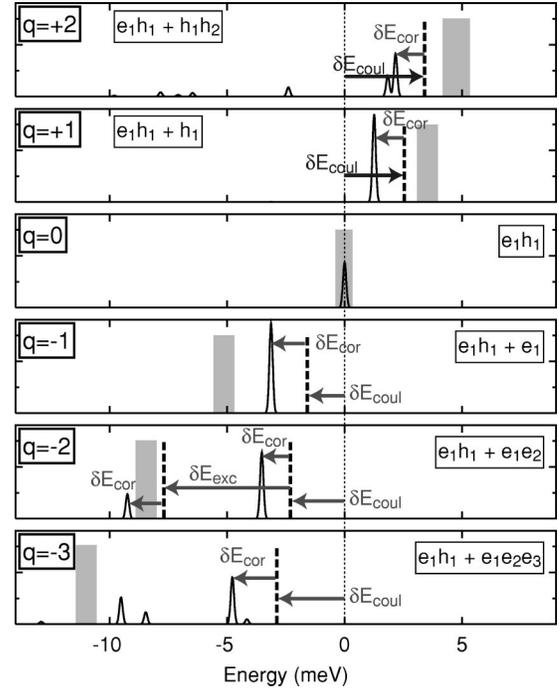

FIG. 5. Comparison between the calculated energy of the e_1-h_1 PL spectral lines (solid lines) and the experimentally measured energy (shaded bars) for various negatively and positively charged QD exciton states. Vertical dashed lines denote calculated peak without correlation. Horizontal arrows show Coulomb, exchange, and correlation shifts. The measured values represent statistical average over 6 different dots from the mixed type sample B. In both experiment and theory the emission energy of negatively charged excitons is lower in energy than that from neutral excitons, while that from positively charged excitons is higher.

arising from the exchange splitting between the triplet and singlet states of the two electrons. The higher energy line which results from the transition to the triplet state is about three times stronger.[8] In the experiment, due to the fact that lines due to few charge states are observed together, only the lowest energy line could be safely identified. (iv) For the $q=-3$ we calculate a multiline PL spectrum, corresponding to the non-Aufbau ($e_1^1 h_1^1$)($e_1 e_2 e_3$) initial state configuration. For the model QD, this configuration is somewhat lower in energy than the Aufbau-like ($e_1^1 h_1^1$)($e_1^1 e_2^2 e_3^0$) initial state since the calculated inter-electronic exchange energy exceeds the single particle energy difference. In the experiment, only a single PL line (X^{-3}) is always observed, indicating that the Aufbau-like state is the lower energy one. We attribute this discrepancy to more than a factor of two overestimated exchange energies (probably due to the above mentioned uncertainties). The influence of near by local charges may also contribute to this discrepancy.

Figure 5 demonstrates a fundamental difference between zero-dimensional charged excitons and those confined in higher-dimensional systems. The negatively charged excitons in our SAQD's, similar to their free charged atomistic analog,[17] have lower recombination energies than their corresponding neutral complexes. Positively charged QD exci-

tons, unlike their analog free positively charged molecules,[17] have larger recombination energies. This novel observation may prove to be very useful in future applications of semiconductor quantum dots, where their optical emission can be discretely varied by controlled carrier injection.

---

[1] M. A. Kastner, Phys. Today **46**, 24 (1993).

[2] R. C. Ashoori, Nature (London) **379**, 413 (1996).

[3] D. Gammon, Nature (London) **405**, 899 (2000).

[4] M. Grundmann, D. Bimberg, and N. N. Ledentsov, *Quantum Dot Heterostructures* (Wiley & Sons, New York, 1998).

[5] W. V. Schoenfeld, T. Lundstrom, P. M. Petroff, and D. Gershoni, Appl. Phys. Lett. **74**, 2194 (1999); T. Lundstrom, W. V. Schoenfeld, H. Lee, and P. M. Petroff, Science **286**, 2312 (1999).

[6] D. L. Klein, R. Roth, A. K. L. Lim, A. P. Alivisatos, and P. L. McEuen, Nature (London) **389**, 699 (1997).

[7] D. Loss and D. P. DiVincenzo, Phys. Rev. A **57**, 120 (1998).

[8] H. Drexler, D. Leonard, W. Hansen, J. P. Kotthaus, and P. M. Petroff, Phys. Rev. Lett. **73**, 2252 (1994); R. J. Warburton, C. Schaflein, D. Haft, F. Bickel, A. Lorke, and K. Karrai, Nature (London) **405**, 926 (2000).

[9] S. Tarucha, D. G. Austing, T. Honda, R. J. van der Hage, and L. P. Kouwenhoven, Phys. Rev. Lett. **77**, 3613 (1996).

[10] U. Banin, Y. Cao, D. Katz, and O. Millo, Nature (London) **400**, 542 (1999).

[11] A. Hartmann, Y. Ducommun, E. Kapon, U. Hohenester, and E. Molinari, Phys. Rev. Lett. **84**, 5648 (2000).

[12] J. J. Finley, A. D. Ashmore, A. Lematre, D. J. Mowbray, M. S. Skolnick, I. E. Itskevich, P. A. Maksym, M. Hopkinson, and T. F. Krauss, Phys. Rev. B **63**, 073 307 (2001).

[13] L. Landin, M. S. Miller, M.-E. Pistol, C. E. Pryor, and L. Samuelson, Science **280**, 162 (1998).

[14] A. Franceschetti and A. Zunger, Phys. Rev. B **62**, 2614 (2000); Europhys. Lett. **50**, 243 (2000).

[15] E. Dekel, D. Gershoni, E. Ehrenfreund, D. Spektor, J. M. Garcia, and P. M. Petroff, Phys. Rev. Lett. **80**, 4991 (1998).

[16] F. Findeis, M. Baier, A. Zrenner, M. Bichler, G. Abstreiter, U. Hohenester, and E. Molinari, Phys. Rev. B **63**, 121 309 (2001).

[17] J. G. Verkade, *A Pictorial Approach to Molecular Bonding* (Springer-Verlag, New-York, 1986).

[18] S. Glasber, S. Finkelstein, H. G. Shtrikman, and I. Bar-Joseph, Phys. Rev. B **59**, R10 425 (1999).

[19] Ph. Lelong and G. Bastard, Solid State Commun. **98**, 819 (1996).

[20] I. N. Stranski and L. Krastanow, Akad. Wiss. Lit. Mainz Abh. Math. Naturwiss. Kl. **146**, 767 (1939).

[21] J. M. Garcia, T. Mankad, P. O. Holtz, P. J. Wellman, and P. M. Petroff, Appl. Phys. Lett. **72**, 3172 (1998).

[22] E. Dekel, D. Gershoni, E. Ehrenfreund, J. M. Garcia, and P. M. Petroff, Phys. Rev. B **61**, 11 009 (2000); E. Dekel, D. V. Regelman, D. Gershoni, E. Ehrenfreund, W. V. Schoenfeld, and P. M. Petroff, *ibid.* **62**, 11 038 (2000).

[23] M. Bayer, O. Stern, P. Hawrylak, S. Fafard, and A. Forchel, Nature (London) **405**, 923 (2000).

[24] R. Rinaldi, S. Antonaci, M. DeVittorio, R. Cingolani, U. Hohenester, E. Molinari, H. Lipsanen, and J. Tulkki, Phys. Rev. B **62**, 1592 (2000).

[25] M. Bayer *et al.*, Phys. Rev. Lett. **82**, 1748 (1999).

[26] M. Kozhevnikov, E. Cohen, A. Ron, H. Shtrikman, and L. N. Pfeiffer, Phys. Rev. B **56**, 2044 (1997).

[27] D. V. Regelman, E. Dekel, D. Gershoni, E. Ehrenfreund, W. V. Schoenfeld, and P. M. Petroff, in *Springer Proceedings in Physics Vol. 87*, proceedings of the 25th International Conference on the Physics of Semiconductors (ICPS25), Osaka, Japan, September 2000, edited by N. Miura and T. Ando (Springer Verlag, Berlin, 2001).

[28] A. Franceschetti and A. Zunger, Phys. Rev. Lett. **78**, 915 (1997).

[29] L.-W. Wang and A. Zunger, Phys. Rev. B **59**, 15 806 (1999).